Non-linear response of solids and nanostructures

Claudio Attaccalite, Davide Sangalli, Myrta Grüning

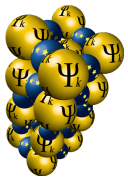

Ψ_k **Scientific Highlight Of The Month**

No. 154 **March 2022**

Non-linear response of solids and nanostructures: a real-time prospective

Claudio Attaccalite[1,2,*], Davide Sangalli[2,3], Myrta Grüning[2,4]

[1] *CNRS/Aix-Marseille Université, Centre Interdisciplinaire de Nanoscience de Marseille UMR 7325 Campus de Luminy, 13288 Marseille cedex 9, France*

[2] *European Theoretical Spectroscopy Facilities (ETSF)*

[3] *CNR-ISM, Division of Ultrafast Processes in Materials (FLASHit), Area della Ricerca di Roma 1, Via Salaria Km 29.3, I-00016 Monterotondo, Scalo, Italy*

[4] *School of Mathematics and Physics, Queen's University Belfast, Northern Ireland, United Kingdom*

Abstract

In recent years many theoretical approaches and computational codes have been developed to study optical response of bulk materials, ranging from many-body perturbation theory to density functional like methods. However the major part of these approaches are limited to the linear optical regime. The few that are formulated in real-time are based on time-dependent density functional theory, an approach where it is difficult to include correlation effects especially for solids. In order to overcome these difficulties some years ago we devised a new real-time computational approach based on dynamical Berry phase plus many-body perturbation theory. This approach is particularly suited to study nonlinear optical properties in crystalline solids and periodic nanostructures. In this highlight we present an introduction to nonlinear optics in solids and how the nonlinear response can be obtained by means of real-time simulations including correlation effects.

*claudio.attaccalite@univ-amu.fr

I. INTRODUCTION TO THE NON-LINEAR OPTICS

A. What is non-linear optics?

When you immerse a solid, either an insulator or a semiconductor, in an electric field (see Fig. 1), the dipoles inside the material get orientated along the field lines and create an internal field, the *polarisation* $\boldsymbol{\mathcal{P}}$, opposite to the field that generates it. This naive picture, even if valid only for finite systems, gives us an idea of the effect of an external electric field on a material. The *total electric field* inside the solid $\boldsymbol{\mathcal{E}}(\mathbf{r},t)$ is the sum of the external plus the polarisation one:

$$\boldsymbol{\mathcal{E}}(\mathbf{r},t) = \boldsymbol{\mathcal{D}}(\mathbf{r},t) - \boldsymbol{\mathcal{P}}(\mathbf{r},t), \qquad (1)$$

where $\boldsymbol{\mathcal{D}}(\mathbf{r},t)$ is the *electric displacement*. This equation is one of the so-called "materials equations", namely the Maxwell equations for electric and magnetic fields in bulk materials. In general one can expand the polarisation $\boldsymbol{\mathcal{P}}$ in a power series of the total electric field $\boldsymbol{\mathcal{E}}$:

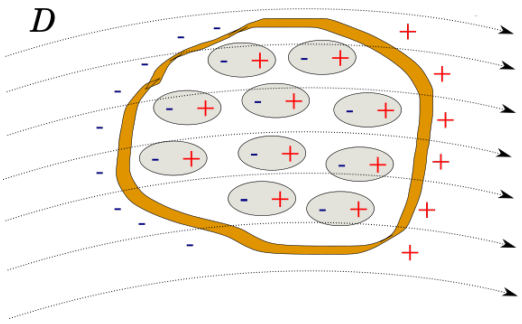

FIG. 1: A solid immersed in an electric field.

$$\boldsymbol{\mathcal{P}} = \boldsymbol{\mathcal{P}}_0 + \chi^{(1)}\boldsymbol{\mathcal{E}} + \chi^{(2)}\boldsymbol{\mathcal{E}}^2 + \chi^{(3)}\boldsymbol{\mathcal{E}}^3 + ... \qquad (2)$$

where $\boldsymbol{\mathcal{P}}_0$ is the intrinsic polarisation of the material at zero electric field, and the coefficients $\chi^{(1)}, \chi^{(2)}, ...$ are response functions of increasing order. Equation 2 is valid for a wide range of situations. However, there are cases where this expansion fails: 1) for very strong fields, beyond the convergence radius of the expansion[1]; 2) when there is an hysteresis, and therefore there is not a univocal relation between polarisation and electric field; 3) close a to phase transitions, where a small external field can drastically change the material properties. In this highlight, we will restrict to the cases in which the expansion in Eq. 2 is valid.

The first term $\chi^{(1)}$ of the power series describes all the phenomena which belong to the linear optics regime. All the other terms $\chi^{(2)}, \chi^{(3)}, ...$ describe the non-linear response, that will be the topic of this highlight.

What does non-linear response mean in practice? We can gain an understanding by rewriting Eq. 2 in frequency domain. For an homogeneous material we obtain:

$$\boldsymbol{\mathcal{P}}(\omega) = \chi^{(1)}(\omega)\boldsymbol{\mathcal{E}}(\omega) + \chi^{(2)}(\omega = \omega_1 + \omega_2)\boldsymbol{\mathcal{E}}(\omega_1)\boldsymbol{\mathcal{E}}(\omega_2) + ... \qquad (3)$$

In the first term (linear regime) on the RHS, the outgoing light [i.e. the polarisation $\boldsymbol{\mathcal{P}}(\omega)$] has the same frequency ω of the incoming one [i.e. the electric filed $\boldsymbol{\mathcal{E}}(\omega)$]. On the contrary, terms beyond the first one contain frequency sum or frequency difference terms, for which the outgoing light has a different frequency (or colour) from the incoming one. For example, in the second harmonic generation (SHG), the outgoing light has a frequency that is twice that of the incoming one.

This effect, despite evident from the equation, is not something we observe in our everyday lives.

In fact, the non-linear coefficients of the polarisation expansion are extremely small. In order to obtain a detectable non-linear response, one needs a sufficiently strong light source. For this reason, the first experimental measurement of second-harmonic generation (SHG) dates 1961[2], a year after the laser invention.[3] In this first experiment of non-linear optics, Franken and his collaborators were able to obtain a SHG signal from a ruby crystal employing a monochromatic laser beam with an intensity of 10^5 volts/cm.
Nowadays lasers with an intensity equivalent to the one used in the Franken's experiment are commercially available in shops and SHG is a common technique to double the laser frequency. Of course, non-linear optics is not limited to the SHG. Nonlinear order terms cover a large spectra of phenomena, such as optical saturation, sum frequency generation, two-photon absorption, generation of higher harmonics. In the next section we will show some applications of non-linear response, and then how these applications can be described from first-principles.

B. What can be done with non-linear optics?

In the last thirty years, the field of non-linear spectroscopy[4] made progresses in leaps and bounds. One of the most common commercial application is the green laser pointer. Many of us uses it when giving slideshow presentations. In this device, the green light is obtained combining a (infra)red laser with a non-linear crystal that doubles the frequency (see Fig. 2). Nowadays non-linear crystals are routinely used in laboratories to change shape, length and intensity of laser beams.
Applications of non-linear optics span a range of disciplines that encompasses condensed matter physics, quantum optics, optoelectronics and medicine.

FIG. 2: Schematic of the green laser pointer.

In biomedical research, SHG is used to probe protein dynamics in biological tissues. In fact, biological tissues does not present a SHG, so nanocrystals with a strong SHG can be bounded to proteins and then inserted in living systems. Under intense illumination, such as the focus of a laser-scanning microscope, these SHG nanocrystals modify the light colour and they can be imaged by means of the two-photon microscopy. Scientists can then visualise the dynamics of the proteins thanks to the nanocrystals. Unlike commonly used fluorescent probes, SHG nanoprobes neither bleach nor blink. The resulting contrast and detectability of SHG nanoprobes provided therefore unique advantages for molecular imaging of living cells and tissues.[5]

In quantum optics, non-linear crystals are used to create entangled photons: a high energy photon is transformed in two (or more) lower energy (entangled) photons by means of reverse

second- or third-harmonic generation. These photons are used in quantum information studies, quantum cryptography or for quantum computation, due to their entangled states.[6]

In condensed matter the non-linear response remains an essential tool to characterise and explore electronic and structural properties of materials. For example, since second-harmonic generation is present only in materials that lack of inversion symmetry, it became a tool to probe phase transitions and phenomena the break this symmetry. Symmetry inversion can be broken in presence of a macroscopic electric field as the one of piezoelectrics, pyroelectrics, and ferroelectrics, or a bulk magnetization as in ferromagnets. Temperature dependent SHG measurement can be used to discriminate between the different phases of these materials.

Another domain where SHG plays a major role is surface spectroscopy. Experimentally, it is non trivial to disentangle bulk and surface contribution from a given signal. SHG is one of the few techniques that can probe the surface, without contributions from the bulk. The reason lies in the fact that in solids with inversion symmetries the bulk has zero SHG signal. This is true not only for bulk materials but also for liquids that are on average symmetric, with the exception of the liquid-liquid or gas-liquid interfaces. SHG is very sensitive to lattice orientation which can be used to characterise surfaces and interfaces and provides great insights on the surface structures, that sometime are difficult to probe with other techniques.[7]

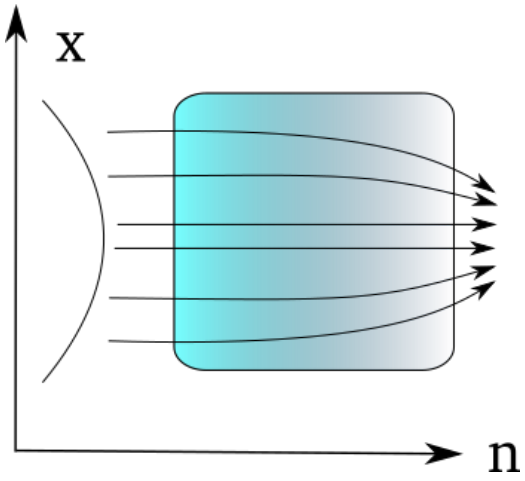

FIG. 3: A schematic representation of the self-focusing phenomena in optical fibers.

Surface SHG spectroscopy techniques have been applied to characterise two-dimensional (2D) material. In a recent experiment,[8] X. Yin et al. used this idea to develop a nonlinear optical imaging technique that allows a rapid and all-optical determination of the crystal orientations in 2D materials at a large scale. Further, Y. Li at al. used SHG to probe the number of layers deposited on a surface, using the fact that an even number of layers posses inversion symmetry while an odd one does not.[9] The importance of non-linear response for materials characterization is not limited to the SHG. Also other response functions find applications in condensed matter physics. For example two-photon absorption, that is proportional to the imaginary part of the $\chi^{(3)}$, can be used to probe excited states that are dark in linear optics.[10,11]

Finally, nonlinear optics effects can be detrimental for some technologies, limiting their application. For example, self-focusing limits the light power that can be transported by optical fibers. Self-focusing is a non-linear optical process seen in materials exposed to intense electromagnetic radiation due to the third-order response χ_3: a medium whose refractive index is significantly modified by the third-order response acts as a focusing lens for an electromagnetic

wave characterised by an initial transverse intensity gradient, as the one generated by a laser beam (see Fig. 3). The peak intensity of the self-focused region keeps increasing as the wave travels through the medium, until medium damage interrupts this process. At present no solution is known for increasing the self-focusing limit in optical fibers[12].
In this introduction we covered a minimal part of the positive and negative non-linear phenomena in research and applications, for a general overview different books and reviews are available in literature.[4][13]

II. HOW TO CALCULATE NON-LINEAR RESPONSE

A. Response-based and real-time approaches

The first calculation of non-linear optical response in solids based on quantum mechanics used a density matrix formalism.[14] The latter formalism had been already used to derive local field effects in linear optics[15][16], to investigate saturation of microwave resonances[17], and to describe nuclear magnetic relaxation[18–20]. One advantage of the density matrix formalism is that effects due to the environment, such as dephasing processes, are easy to include.[21]

The density matrix formalism is based on the solution of the Liouville-von Neumann equation[22] for the electronic one-body reduced density-matrix ρ:

$$i\hbar\frac{\partial\rho}{\partial t} = [\mathbf{H}_A, \rho] + [\mathbf{H}_{coh}, \rho] + i\hbar\left(\frac{\partial\rho}{\partial t}\right)_{damping}. \tag{4}$$

The right-hand side of this equation of motion (EOM), Eq. 4, contains three terms. $\mathbf{H}_A$ describes the unperturbed energy levels of the system, $\mathbf{H}_{coh}$ describes the coupling with the external perturbation—which in the case of nonlinear response calculations, is a monochromatic ever lasting electro-magnetic field—and finally $(\partial\rho/\partial t)_{damping}$ introduces decoherence and relaxation processes.

Decoherence is due to the interaction with other degrees of freedom—for example the vibrations of the lattice, or phonon modes—and other environmental effects. The coupling with the environment can be modeled, for example, by introducing a $\mathbf{H}_{random}$ Hamiltonian which accounts for random processes.[21]
If one wants to include electron-electron interaction in the EOM [Eq. 4] static electron correlation can be accounted by a term which has the form $[\Sigma^{xc,static}, \rho]$, thus affecting the electronic structure of the system, while dynamical correlation is included as an additional relaxation process in the $(\partial\rho/\partial t)_{damping}$ term.

A steady-state solution for Eq. 4 in ascending powers of the coupling term may be found from the following hierarchy equations:

$$i\hbar\frac{\partial\rho^{(0)}}{\partial t} = [\mathbf{H}_A, \rho^{(0)}] + i\hbar\left(\frac{\partial\rho^{(0)}}{\partial t}\right)_{damping}, \tag{5}$$

$$i\hbar\frac{\partial\rho^{(1)}}{\partial t} = [\mathbf{H}_A, \rho^{(1)}] + [\mathbf{H}_{coh}, \rho^{(0)}] + i\hbar\left(\frac{\partial\rho^{(1)}}{\partial t}\right)_{damping}, \tag{6}$$

$$i\hbar\frac{\partial\rho^{(2)}}{\partial t} = [\mathbf{H}_A, \rho^{(2)}] + [\mathbf{H}_{coh}, \rho^{(1)}] + i\hbar\left(\frac{\partial\rho^{(2)}}{\partial t}\right)_{damping}. \tag{7}$$

The first equation gives the density matrix at equilibrium. The second equation describes the linear response. By Fourier analysis it is easy to show that $\rho^{(1)}$ must contain the same frequencies as $\mathbf{H}_{coh}$. The $\rho^{(2)}$ is the first non-linear term. Differently from $\rho^{(1)}$, $\rho^{(2)}$ oscillates at a frequency that can be the sum or difference of the incoming fields. This term describes for example, second harmonic generation and optical rectification. Higher order terms $\rho^{(n)}$, describes for example, higher harmonic generations and saturation phenomena.

From these hierarchy equations, it is possible to derive the corresponding Dyson-like equations for the response functions $\chi^{(1)}$, $\chi^{(2)}, \ldots$ by differentiating the density matrix respect to the external perturbation. Alternatively, expressions for nonlinear response functions can be also derived directly from perturbation theory.[23–25]

The standard solution of the Dyson equations for the response functions and their corresponding implies a sum-over-states (i.e. valence and conduction bands times k-points) which allows for an interpretation of the features in the nonlinear responses in terms of the electronic structure, but it quickly become computationally heavy as the number of bands and k-points increases. For this reason, alternative approaches to calculate non-linear response functions has been developed. For example, Dal Corso and Mauri used the "2n+1" theorem in the time-dependent density functional theory (TDDFT) framework to calculate static nonlinear susceptibilities avoiding the sum over states.[26] Others, used a frequency-dependent Sternheimer equation to obtain dynamic polarisabilities and hyperpolarizabilities in molecular systems.[27]

Another approach consists of directly integrating the EOM in Eq. 4 and then analysing the outgoing polarisation or current. This approach is referred to as real-time solution. It has a better scaling with the system size than response-based approaches and allows for calculating the response at all orders within the same calculation and to go beyond the perturbative regime. Nevertheless, real-time approaches has not been very popular, mostly for two reasons. First, though the real-time solution scales better with the system size, it has a large prefactor so that effectively it is cheaper than response-based approaches only for very large systems; second, the analysis of the results is more cumbersome compared to response-based approaches. In last decades, however, real-time approaches have been used in several works to calculate non-linear response both for molecular[28,29] and periodic systems.[30]

B. Electronic structure and correlation effects

The first calculations of non-linear response were often underestimating or overestimating the experimental values by one or two order of magnitudes.[31,32] These large differences were due the use of empirical pseudo-potentials to calculate the electronic structure and to the neglection of correlation effects.

In the nineties, Levine[24] presented for the first time an *ab-initio* formalism for the calculation of the second-harmonic generation. Sipe and coworkers extended the calculation of non-linear response to the third harmonic generation[33,34] (eliminating unphysical divergences that are present in the velocity gauge). Calculations based on ab-initio electronic structures greatly improved results over empirical approaches. Few years later, Levine and coworkers performed the first calculations of the second harmonic generation beyond the independent-particle approximation, including local-field effects and self-energy effects by means of a scissor

operator.[23,35]

A few works, included electron-hole interaction, thus excitonic effects, in the non-linear response. Within Green's function theory, excitonic effects can be included by generalising the Bethe-Salpeter equation (BSE)[36] to higher order response functions. Chang et al.[37] and Leitsman et al.[38] proposed an *ab-initio* many body framework for computing the frequency dependent second-harmonic generation that includes local fields and excitonic effects through an effective two-particle Hamiltonian derived from the BSE and obtained a good agreement with the experimental results. More recently, Hubener[39] proposed a full Bethe-Salpeter equation for the second-order response functions, while Virk and Sipe derived a similar approach for the third-harmonic generation.[40] The latter approaches are including high-order correlations beyond the standard BSE approach. However, at present these approaches have not been applied to real-materials.

Time-Dependent Density Functional Theory (TDDFT)[41] represents a possible alternative to the formalism based on Green's function. TDDFT is in principle an exact theory to calculate response functions in finite systems. However, the exchange-correlation functional that enters in the equations is unknown and has to be approximated. Standard approximations that rely on local or semi-local functionals miss long range contributions that are responsible of excitonic effects[42]. Nevertheless, in its real-time formulation, in velocity gauge, TD-DFT at the level of standard approximation for the exchange-correlation functional has been used to calculate non-linear response functions of both finite and extended systems providing very good results for the systems under study.[27,28]

Long range contribution can be included in a reciprocal or real-space either empirically or through hybrid functionals.[42] Recently, E. Luppi et al. extended the TD-DFT formalism to the calculation of second-harmonic generation including local field and excitonic effect.[25] However, this promising approach[43] is limited by the treatment of the electron correlation to systems with weakly bound excitons.[44]

III. DYNAMICAL BERRY'S PHASE AND NON-LINEAR RESPONSE

In the previous section, we discussed the advantages of frequency-response derived from the density matrix EOMs, Eq. 4, over real-time approaches that integrate directly Eq. 4. We have also discussed the progress in accounting for electron correlation. In fact, within Green's function theory the inclusion of many-body effects into the expression for the nonlinear optical responses is extremely cumbersome. Furthermore the complexity of these expressions grows with the perturbation order. Therefore it is not surprising that there have been only few isolated attempts of including electron correlation at this level of theory.

Real-time approaches present the major advantage that electron correlation can be included straightforwardly by adding many-body operators to the Hamiltonian. A further advantage of real-time approaches is that they are non-perturbative in the external fields and therefore one obtains optical susceptibilities at any order without increasing the computational cost and with the only limitation dictated by the machine precision. Finally, within a real-time approach, several non-linear phenomena and thus spectroscopic techniques are described by the same EOMs. For instance, by the superposition of several laser fields one can simulate sum- and difference-frequency harmonic generation, or four-waves mixing.[13] On the other hand, within a real-time density matrix formalism describing the coupling between light and electrons in extended periodic system is far from straightforward.

Here, we present a real-time *ab-initio* approach based on a formalism alternative to density matrix and based on an effective Schrödinger equation where the coupling between light and electrons in a periodic system is derived from the Berry's dynamical polarisation following the scheme proposed by Souza et al.[45]. Before presenting the approach, we briefly discussed the definition of polarisation in periodic systems. In our approach, we introduce correlation both within the Green's function theory, producing the real-time equivalent of the BSE and within a TD-DFT framework.

A. Why do we need Berry's phase?

For many years, the correct definition of polarisation in periodic systems remained an unsolved problem in solid state physics. Over the years, different wrong definitions of bulk polarisation have been proposed in the literature (see a review in Ref.[46]). The definition of polarisation is intrinsically related to the one of the dipole operator, that is a problematic object for extended systems. In crystalline solids, the definition of bulk polarisation is difficult for two main reasons. First, in treating crystalline solids one imposes periodic boundary conditions to reflect the periodicity of the lattice and the Bloch functions. With periodic boundary conditions, the position operator, that is not periodic, is ill-defined. Then, a definition of the dipole operator, and thus of the polarizability, that relies on the position is ill-defined.Second, differently from finite systems, the polarisation cannot be expressed as an integral on the charge density[47]. This can be understood when we write down the general relation between polarisation and density:

$$\nabla \cdot \mathbf{P}(\mathbf{r}) = -n(\mathbf{r}), \tag{8}$$

which, for a periodic system, can be written in terms of the Fourier components of $\mathbf{P}$ and n, where $\mathbf{G}$ denotes a reciprocal lattice vector and $\mathbf{q}$ belongs to the first Brillouin zone(BZ), as:

$$(\mathbf{q}+\mathbf{G})\cdot\mathbf{P}(\mathbf{q}+\mathbf{G}) = in(\mathbf{q}+\mathbf{G}). \tag{9}$$

It follows from Eq. 9 that each Fourier component can be treated separately. Now let us consider the limit $\mathbf{q}\to 0$ for $\mathbf{G}=0$: the macroscopic polarisation $\mathbf{P}$ is not determined by the zero Fourier component of the density, which must vanish by charge neutrality. In finite systems, this is fixed by the condition $\mathbf{P}(\mathbf{r})\to 0$ outside the sample (Dirichlet boundary condition). Instead in an infinite crystal, in the limit $\mathbf{q}=0$, the polarisation contains additional information not included in the density.[47] A correct definition of polarisation in periodic systems was proposed in 1993 by King-Smith and Vanderbilt,[48] and later refined by Resta.[49,50] In their seminal paper, King-Smith and Vanderbilt showed that the bulk polarisation can be expressed as a closed integral in the Brillouin zone on the wave-function phase, a particular case of the Berry's phase. Their formulation solved all problems with the previous attempts to define the polarisation. In fact the King-Smith and Vanderbilt polarisation is a bulk quantity, its time derivative gives the current and its derivatives respect to the external field reproduce the polarisabilities at all orders.

B. Bulk polarization and response functions

1. *Treatment of the field coupling term and equations of motion*

We sketch the derivation of the EOMs for electrons in a periodic potential coupled with an external electric field in length gauge. We start from the macroscopic bulk polarisation, in terms of the many-body geometric (Berry) phase, as defined in the Modern Theory of Polarisation[50],

$$\mathbf{P}_\alpha = \frac{eN_{\mathbf{k}_\alpha}\mathbf{a}_\alpha}{2\pi V}\mathrm{Im}\ \ln\ \langle\Psi_0|\mathrm{e}^{i\mathbf{q}_\alpha\cdot\hat{\mathbf{X}}}|\Psi_0\rangle. \tag{10}$$

In Eq. (10) $\mathbf{P}_\alpha$ is the macroscopic polarisation along the primitive lattice vector $\mathbf{a}_\alpha$, $\hat{\mathbf{X}} = \sum_{i=1}^{N}\hat{\mathbf{x}}_i$, $\mathbf{q}_\alpha = \frac{\mathbf{b}_\alpha}{N_{\mathbf{k}_\alpha}}$ with $\mathbf{b}_\alpha$ the primitive reciprocal lattice vector such that $\mathbf{b}_\alpha\cdot\mathbf{a}_\alpha = 2\pi$, and $N_{\mathbf{k}_\alpha}$ the number of $\mathbf{k}$-points along α, corresponding to the number of equivalent cells in that direction, $\mathbf{q}_\alpha$ is the smallest distance between two k-points along the α direction. Note that in this formulation the polarisation operator is a genuine many-body operator that cannot be split as a sum of single-particle operators.

The polarization defined by the Eq. 10 is valid for any many-body wave-function on lattice or continuum[49,51]. This expression can be simplified in case the full many-body wave-function Ψ_0 can be written as a single Slater determinant. In this case, the expectation value of the many-body geometric phase in Eq. (10) can be written in terms of overlaps between two single Slater determinants at adjacent k-points.[51]

$$\mathbf{P}_\alpha = -\frac{ef}{2\pi v}\frac{\mathbf{a}_\alpha}{N_{\mathbf{k}_\alpha^\perp}}\sum_{\mathbf{k}_\alpha^\perp}\mathrm{Im}\sum_{i=1}^{N_{\mathbf{k}_\alpha}-1}\ \mathrm{tr}\ \ln\ S(\mathbf{k}_i,\mathbf{k}_i+\mathbf{q}_\alpha) \tag{11}$$

where $S_{mn}(\mathbf{k},\mathbf{k}+\mathbf{q}_\alpha) = \langle v_{\mathbf{k},m}|v_{\mathbf{k}+\mathbf{q}_\alpha,n}\rangle$ is the overlaps matrix between the wave-function at $\mathbf{k}$ and $\mathbf{k}+\mathbf{q}$.

Next, we consider the Lagrangian of the system in presence of an external electric field $\boldsymbol{\varepsilon}$,[45]

$$\mathcal{L} = \frac{i\hbar}{N_{\mathbf{k}}} \sum_{n=1}^{M} \sum_{\mathbf{k}} \langle v_{\mathbf{k}n} | \dot{v}_{\mathbf{k}n} \rangle - E^0 - v\boldsymbol{\varepsilon} \cdot \mathbf{P}, \tag{12}$$

where E^0 is the energy functional corresponding to the zero-field Hamiltonian $\hat{H}^0$, and the last term $v\boldsymbol{\varepsilon} \cdot \mathbf{P}$ is the coupling between the external field and the polarization.
Finally, from Eq. 12 we obtain the Euler-Lagrange equations of motion:[45]

$$i\hbar \frac{d}{dt} |v_{\mathbf{k},m}\rangle = \left(\hat{H}^0_{\mathbf{k}} + \hat{w}_{\mathbf{k}}(\boldsymbol{\varepsilon}) + \hat{w}^{\dagger}_{\mathbf{k}}(\boldsymbol{\varepsilon}) \right) |v_{\mathbf{k},m}\rangle. \tag{13}$$

The field coupling operator $\hat{w}_{\mathbf{k}}(\boldsymbol{\varepsilon})$ contains a term proportional to $\frac{1}{2\Delta\mathbf{k}_\alpha} \left(|\tilde{v}_{\mathbf{k}^+_\alpha,n}\rangle - |\tilde{v}_{\mathbf{k}^-_\alpha,n}\rangle \right)$ that has the form of the two-points central finite difference approximation with grid spacing $\Delta\mathbf{k}_\alpha$ of $\tilde{\partial}_{\mathbf{k}_\alpha} |v_{\mathbf{k}_\alpha}\rangle$ the covariant partial derivative with respect to the crystal momentum of the Bloch function. The $|\tilde{v}_{\mathbf{k}^\pm}\rangle$ (where the $\mathbf{k}^\pm$ stands for $\mathbf{k} \pm \Delta\mathbf{k}$) are built from the $|v_{\mathbf{k}^\pm}\rangle$ in such a way that they transform as $|v_{\mathbf{k}}\rangle$ under a unitary transformation $U_{\mathbf{k},nn'}$ and so the derivative is well defined.[45]

2. *Treatment of electron correlation*

Correlation effects play a crucial role in both linear[52] and non linear[25,53] response of solids. It is recognised that beyond the independent-particle approximation (IPA), for an accurate prediction of optical properties, one needs to include local-field and excitonic effects and quasi-particle corrections. In the framework of Green's function theory, a very successful way to deal with electron-electron interaction in semiconductors is the combination of the G_0W_0 approximation for the quasi-particle band structure[54] with the Bethe-Salpeter equation (BSE) in static ladder approximation for the response function.[36] Other approaches, such as time-dependent density functional theory and time-dependent Hartree-Fock are not suitable approaches to optical properties of dielectrics. The former, within standard approximations for the exchange-correlation approximations, underestimates the optical gap and misses the excitonic resonances; the latter largely overestimates the band-gap and excitonic effects.

Working within non-equilibrium Green's function theory, we extended the BSE approach to the real-time domain[55] and derived a single-particle Hamiltonian that includes correlation from Green's function theory, and as its response-based counterpart includes correlation effects relevant for optical response. Furthermore, since we neglected dynamic correlation, the solution of the single-particle Hamiltonian can be written as a single Slater determinant, as assumed in Eq. (10). In what follows, we start from the IPA, and add gradually the relevant corrections and effects to the Hamiltonian in Eq. 13, providing an overview of the levels of theory included in the formalism.

The starting point for our real-time dynamics is the Kohn-Sham Hamiltonian at fixed density as a system of independent particles,[56]

$$\hat{H}^{0,\mathrm{IPA}} \equiv \hat{h}^{\mathrm{KS}} = -\frac{\hbar^2}{2m} \sum_i \nabla_i^2 + \hat{V}_{eI} + \hat{V}_H[n_0] + \hat{V}_{\mathrm{xc}}[n_0], \tag{14}$$

where V_{eI} is the electron-ion interaction, V_H the Hartree potential, $V_{\rm xc}$ the exchange-correlation potential and n_0 is the equilibrium electronic density. The advantage of such a choice is that the Kohn-Sham system is the independent-particle system that reproduces the electronic density of the unperturbed many-body interacting system ρ^0, thus by virtue of the Hohenberg-Kohn theorem[57] the ground-state properties of the system. Furthermore, no material dependent parameters need to be input, but for the atomic structure and composition.

As first step beyond the IPA, we introduce the corrections to the independent-particle energy levels by the electron-electron interaction through a (state-dependent) scissor operator

$$\Delta\hat{H} = \sum_{i,\mathbf{k}} \Delta_{i,\mathbf{k}} |v^0_{i,\mathbf{k}}\rangle\langle v^0_{i,\mathbf{k}}|. \tag{15}$$

The latter can be calculated *ab-initio* e.g., via the G_0W_0 approach $\Delta_{i,\mathbf{k}} = (E^{G_0W_0}_{i,\mathbf{k}} - \varepsilon^{\rm KS}_{i,\mathbf{k}})$, or can be determined empirically from the experimental band gap $\Delta_{i,\mathbf{k}} = \Delta = E^{\rm exp}_{\rm GAP} - \Delta\varepsilon^{\rm KS}_{\rm GAP}$. We refer to this approximation as the independent quasi-particle approximation (QPA):

$$\hat{H}^{0,\rm QPA} \equiv \hat{h}^{\rm KS} + \Delta\hat{H}. \tag{16}$$

Notice that in our approach the inclusion of a non-local operator in the Hamiltonian does not present more difficulties than a local one, while this is not a trivial task in the response theory in frequency domain[25]. As a second step we consider the effects originating from the response of the effective potential to density fluctuations. By considering the change of the Hartree plus the exchange-correlation potential in Eq. 14 we will obtain the TD-DFT response. Here we include just "classic electrostatic" effects via the Hartree part. We refer to this level of approximation as the time-dependent Hartree (TDH)

$$\hat{H}^{0,\rm TDH} \equiv \hat{H}^{0,\rm QPA} + \hat{V}_H[n - n_0]. \tag{17}$$

In the linear response limit the TDH is usually referred as Random-Phase approximation and is responsible for the so-called crystal local field effects.[15]

Beyond the TDH approximation one has the TD-Hartree-Fock that includes the response of the exchange term to fluctuations of the density matrix ρ. As discussed above this level of approximation is insufficient for optical properties of semiconductors, normally worsening over TDH results. The next step is thus to consider a screened exchange term in which the relevant electron correlation is introduced as a static screening term.[36] The latter is calculated for the unperturbed KS system and is fixed to its initial value. We refer to this level of approximation as TD-BSE, also known in other works as TD screened Hartree-Fock (TD-SHF):

$$\mathbf{H}_{mb}(t) = \mathbf{h}_{\mathbf{k}} + \Delta\mathbf{h}_{\mathbf{k}} + \mathbf{U}_{\mathbf{k}} + \mathbf{V}^H_{\mathbf{k}}[n - n_0] + \mathbf{\Sigma}^{\rm cohsex}_{\mathbf{k}}[\rho - \rho_0]. \tag{18}$$

where $\mathbf{\Sigma}^{\rm cohsex}_{\mathbf{k}}[\rho - \rho_0]$ is the screened exchange self-energy[55], an example of the static correlation $\mathbf{\Sigma}^{xc,static}$ mentioned in the introduction. ρ_0 is the equilibrium density matrix, that can be reconstruct from the time-dependent valence bands.[58]

We want to emphasize again that within this approach many-body effects are easily implemented by adding terms to the unperturbed independent-particle Hamiltonian $\hat{H}^{0,\rm IPA}$ in the EOMs [Eq. (13)]. Limitations may arise because of the computational cost of calculating those additional terms. For instance, the large number of $\mathbf{k}$-points needed to converge the SHG and THG spectra can hinder calculations of these spectra at this level of theory for some material.

When the wave-function cannot be approximated anymore with a single Slater determinant (as in strong-correlated systems) the evaluation of the polarisation operator [Eq. 10] becomes quite cumbersome.[59] Also we are not aware of any successful attempt to combine Berry's phase polarisation with Green's function theory or density matrix kinetic equations beyond the screened Hartree-Fock approximation (i.e. including scattering terms), even if some appealing approaches have been proposed in the literature[60–63].
Notice that all correlation terms we included in the Hamiltonian, Eq. 18, are Hermitian and static, therefore they do not provide any dephasing effect in the dynamics. In order to describe dephasing due to electronic correlation, scattering with phonons and broadening from other sources, we included a phenomenological non-Hermitian operator as described in Ref. 58. The latter approach to include dephasing effects are formally correct for non-interacting electrons. A proper formulation of dephasing beyond the IPA is instead far from trivial within single particle approaches (either density-matrix or wave-function based).[64]

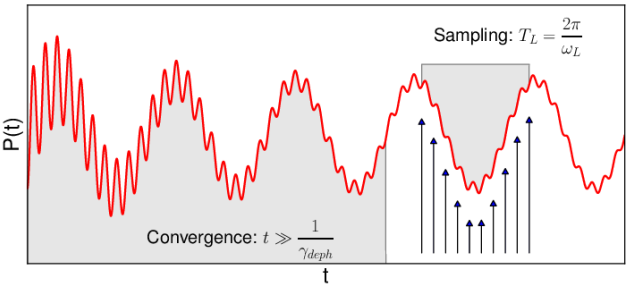

FIG. 4: Pictorial representation of the signal analysis in the post-processing step. The signal $P(t)$ (red line) can be divided into two regions: an initial convergence region (up to $t \gg 1/\gamma_{deph}$) in which the eigenfrequencies of the systems are "filtered out" by dephasing. In this second region the signal $P(t)$ is sampled within a period $T_L = 2\pi/\omega_L$ to extract the $\mathbf{p}_n$ coefficients.

3. *Density-polarization functional theory formulation*

As discussed previously, the time-dependent density functional theory (TDDFT) is an approach to calculate optical properties beyond the IPA. TDDFT is an extension of the ground-state formalism that allows to investigate the properties and dynamics of many-body systems in the presence of time-dependent potential.[41] TDDFT has been applied successfully in molecular systems. In contrast with other approaches, as for instance Green's function theory[36] that provides a similar accuracy in extended[65] and finite systems[66], results obtained within standard TDDFT for dielectrics has an accuracy similar to the Random Phase Approximation. On the other hand, TDDFT has a much lower cost than the Green's function formalism and it is therefore appealing to develop TDDFT approaches that, maintaining the computational costs of standard approximations, can provide accurate optical spectra of dielectrics. While much of the attention in the literature is dedicated to the development of approximations for the exchange-correlation potential—that effectively describes many-body effects within DFT, the issue of TDDFT in solids is of fundamental nature. The central proof of TDDFT, demonstrating the mapping between the time-dependent density and the time-dependent potential, relies on the mapping between currents and densities through the continuity equation. This mapping requires a surface integral involving the density and the potential to vanish. For finite systems, this condition is satisfied rigorously. For a periodic system, the condition can be satisfied as long as the density and potential are periodic. When a macroscopic uniform electric field

is applied and the potential is no longer periodic, there is no mapping between density and current-density and TDDFT does not apply.[67] This is exactly the case when we try to calculate optical properties by using TDDFT.

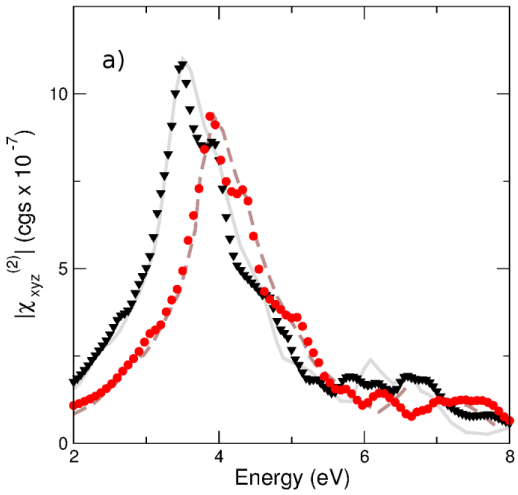

FIG. 5: Magnitude of $\chi^{(2)}(-2\omega, \omega, \omega)$ for bulk SiC calculated within the IPA (black triangles) and QPA (red circles). Each point corresponds to a real-time simulation at the given laser frequency. Comparison is made with results obtained *ab-initio* by direct evaluation of the $\chi^{(2)}$ in Ref.[25] in IPA (grey solid line) and QPA (brown dashed line).

A nice illustration of this fundamental problem is given in the paper of Maitra et. al.[68] through the example of a free electron gas on a ring subjected to a constant uniform electric field. For this simple system, it is possible to write down the exact solution: one finds that the electric field modifies only the phase of the single particle orbitals, leaving the density unchanged. Then different electric fields give rise to exactly the same density and therefore there is not an unique mapping between the density and the (macroscopic) external field. The problem can be overcome considering instead the mapping of the macroscopic external field with current density. In fact, an extension of TDDFT, Time-Dependent Current Density Functional Theory (TD-CDFT)—that maps directly the external potential and the current-density—was proposed at by Ghosh and Dhara in the late eighties[69].

An alternative to the current density based TD-CDFT is the density and polarization based time-dependent density and polarization functional theory (TDDPFT). In the latter approach, one uses the relation between polarisation and current to construct a theory that relies on density and polarization instead of current density. The use the polarisation as an additional to the density is a valid approximation when the transverse microscopic contribution of the current is negligible. In the case of the optical response in the limit of long-wave length limit, this is a valid approximation. Within the TDDFTP the Hamiltonian reads:

$$H^s_{\mathbf{k}} = -\frac{1}{2}\left(\nabla + i\mathbf{k}\right)^2 + \bar{v}^s(\mathbf{r}) - \Omega\boldsymbol{\mathcal{E}}^s \cdot \nabla_{\mathbf{k}} \tag{19}$$

which is a functional of both the density and the polarisation and $\boldsymbol{\mathcal{E}}^s$ is the Kohn-Sham (KS) macroscopic field, that contains the corresponding macroscopic components of the exchange correlation functional. The KS macroscopic electric field can be parameterised in different way, starting from long-range corrected functionals, imposing the exact constraint in the linear response limit. We tested and implemented different possible approximations for the KS macroscopic electric field, see Refs. 70 and 71.

4. Non-linear response functions from real-time simulations

A real-time simulation outputs the real-item polarisation. Similarly to an experiment, we can change the intensity and temporal behavior of the external field and the signal post-processing to

obtain the response function of interest. For example in the second/third harmonic generation case, we perturb the system with a monochromatic electric field $\boldsymbol{\varepsilon}(t) = \boldsymbol{\varepsilon}_0 \sin(\omega_L t)$, where ω_L is the frequency of the external perturbation. Once, due to decoherence, the amplitude of the eigenemodes of the system becomes negligible, the polarisation $\mathbf{P}(t)$ is a periodic function of period $T_L = \frac{2\pi}{\omega_L}$ and can be expanded in a Fourier series as:

$$\mathbf{P}(t) = \sum_{n=-\infty}^{+\infty} \mathbf{p}_n e^{-in\omega_L t}, \tag{20}$$

where the complex coefficients $\mathbf{p}_n$ are proportional to the n^{th}-harmonic-generation response at ω_L. These coefficients can be obtained by solving the set of linear equations resulting when Eq. 20 is truncated at some order N and evaluated at $2N+1$ times t sampled as shown in Fig. 4. To obtain the frequency-dependent n^{th}-harmonic-generation response, one runs a set of simulations sweeping ω_L over the range of frequencies of interest.

A different scheme is used to study the two-photon absorption. Two-photon absorption is given by the third-order response function at the same frequencies of the incoming laser. In this case, for a given laser frequency, we perform simulations at different laser intensities and we resort to a Richardson extrapolation to extract the contribution we are interested in.[72]

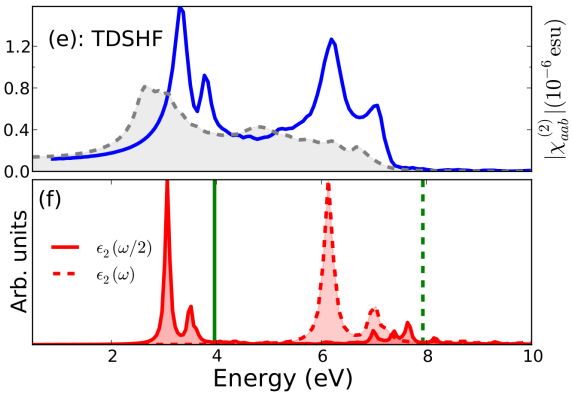

FIG. 6: SHG spectra for the h-BN monolayer at different levels of theory [Eq. (18)]: (a) IPA (dashed grey line) and TD-BSE (continuous blue line). The imaginary part of the dielectric constant at both $\omega/2$ (red continuous line) and ω (red dashed line) is reported in (b) at the TD-BSE level. The vertical lines represent the *GW* fundamental gap (green dashed line) and half of the *GW* fundamental gap (green continuous line).

C. Results

The computational scheme presented in previous sections has been used to calculate nonlinear properties in a range of systems.

First, the computational approach has been validated by direct comparison with existing calculations in frequency domain for bulk semiconductors. For example in Fig. 5 we compare SHG in SiC calculated from real-time simulations against the results of Refs.[25,73]. An almost perfect agreement between the two approaches was found. Similar comparison has been performed also for third harmonic generation against simple models and against experimental results, see Ref. 58.

The approach has been used particularly for 2D and layered materials[74–78] for which non-linear optical properties are dominated by strongly bound excitons, that as discussed previously are not captured by other approaches. As an example, we show the non-linear response of h-BN. In Fig. 6 we report the calculated absolute value of $\chi^{(2)}_{aab}(\omega)$ at different levels of approximation. At IPA level, the SHG presents a peak at 2.3 eV and a broad structure between $4-7eV$. When we turn on correlation effects using the full Hamiltonian, Eq. (18), the results change completely.

Excitonic effect enhance the non-linear response and compensate the quasi-particle corrections. By comparing with the imaginary part of the dielectric constant ϵ_2 both at $\omega/2$ and ω [Fig. 6] calculated at the same level of theory, the two couples of peaks can be identified respectively as the two- and one-photon resonances with the excitons at 6 and 7 eV. Excitonic effects has been studied also for the two-photon absorption in single layered and bulk h-BN and for the third-harmonic generation of one-dimensional systems, see Ref. 72 and 79. In the latter case, adding quasiparticle corrections and excitonic effects leads again to a very different spectra when compared to the independent particle case. In particular, there is a strong redistribution of the intensity over a broader range of frequencies, with the net result of a reduced intensity of the main peak with respect to the IPA.
SHG spectrum of semiconductors have been treated as well within the TD-DPFT framework[25] by using the so-called long-range-corrected (LRC) approximation,[44] a semi-empirical simple model for the screened electron-hole attraction, that includes only the long-range part of the interaction. As earlier recognised, this approximation fails for strong excitons. In fact by tuning the empirical parameter for the screening we could get the position of the first exciton, though its intensity is strongly overestimated (see caption of Fig. 6), but in no way we could get the second excitonic peak. Those pitfalls reflected also in the SHG spectrum, as shown in Refs.[70,71].

IV. CONCLUSIONS

In this highlight we presented an *ab-initio* real-time approach to calculate nonlinear optical properties of extended systems in the length gauge. The key strengths of the proposed approach are first, the correct treatment of the coupling between electrons and the external field and second the possibility to include easily static correlation effects beyond the IPA. This approach is implemented in the Yambo code[80] and different tutorials are available on how to calculate the non-linear response.[81] The code is open-source and freely available.The code avails of the sophisticated parallelization of the yambo code[80] and allows to parallelize the simulations on frequencies and **k**-points.

Although very accurate for the non-linear response, our approach is missing dynamic correlation effects, to accurately describe scattering and decoherence, processes and correlation effects beyond electron-hole interaction, as for example those needed to describe bi-excitons or trions.[82] Furthermore, calculation of non-linear response in complex system can be challenging due to the computational and memory requirements. There are several on-going efforts to extend the approach and overcome some of its limitations, for example, 1) the extension to pump and probe spectroscopies; 2) the inclusion of temperature effects by considering an electron-phonon self-energy; 3) the application to non-perturbative phenomena as high-harmonic generation.

[1] K.-M. Lee, C. M. Kim, S. A. Sato, T. Otobe, Y. Shinohara, K. Yabana, and T. M. Jeong, Journal of Applied Physics **115**, 053519 (2014).

[2] P. Franken, A. Hill, C. e. Peters, and G. Weinreich, Physical Review Letters **7**, 118 (1961).

[3] T. H. Maiman, SPIE milestone series , 61 (1960).

[4] N. Bloembergen, Reviews of Modern Physics **54**, 685 (1982).

[5] P. Pantazis, J. Maloney, D. Wu, and S. E. Fraser, Proceedings of the National Academy of Sciences **107**, 14535 (2010).

[6] P. G. Kwiat, K. Mattle, H. Weinfurter, A. Zeilinger, A. V. Sergienko, and Y. Shih, Phys. Rev. Lett. **75**, 4337 (1995).

[7] K. Eisenthal, Chemical Reviews **96**, 1343 (1996).

[8] X. Yin, Z. Ye, D. A. Chenet, Y. Ye, K. O'Brien, J. C. Hone, and X. Zhang, Science **344**, 488 (2014).

[9] Y. Li *et al.*, Nano Letters **13**, 3329 (2013).

[10] F. Wang, G. Dukovic, L. E. Brus, and T. F. Heinz, Science **308**, 838 (2005).

[11] G. Cassabois, P. Valvin, and B. Gil, arXiv preprint arXiv:1512.02962 (2015).

[12] R. Photonics, "The encyclopedia of laser physics and technology," .

[13] R. W. Boyd, *Nonlinear Optics* (Academic Press, 2008).

[14] N. Bloembergen and Y. Shen, Physical Review **133**, A37 (1964).

[15] S. L. Adler, Phys. Rev. **126**, 413 (1962).

[16] N. Wiser, Physical Review **129**, 62 (1963).

[17] R. Karplus and J. Schwinger, Physical Review **73**, 1020 (1948).

[18] R. Kubo and K. Tomita, Journal of the Physical Society of Japan **9**, 888 (1954).

[19] P. S. Hubbard, Rev. Mod. Phys. **33**, 249 (1961).

[20] F. Bloch, Phys. Rev. **102**, 104 (1956).

[21] D. Manzano, Aip Advances **10**, 025106 (2020).

[22] J. Von Neumann, Nachrichten von der Gesellschaft der Wissenschaften zu Göttingen, Mathematisch-Physikalische Klasse **1927**, 245 (1927).

[23] J. Chen, L. Jönsson, J. W. Wilkins, and Z. H. Levine, Phys. Rev. B **56**, 1787 (1997).

[24] Z. H. Levine, Phys. Rev. B **42**, 3567 (1990).

[25] E. Luppi, H. Hübener, and V. Véniard, Phys. Rev. B **82**, 235201 (2010).

[26] A. Dal Corso and F. Mauri, Phys. Rev. B **50**, 5756 (1994).

[27] X. Andrade, S. Botti, M. A. Marques, and A. Rubio, The Journal of chemical physics **126**, 184106

(2007).

[28] Y. Takimoto, F. D. Vila, and J. J. Rehr, The Journal of Chemical Physics **127**, 154114 (2007).

[29] F. Ding, B. E. Van Kuiken, B. E. Eichinger, and X. Li, The Journal of chemical physics **138**, 064104 (2013).

[30] V. A. Goncharov, The Journal of chemical physics **139**, 084104 (2013).

[31] C. Y. Fong and Y. R. Shen, Phys. Rev. B **12**, 2325 (1975).

[32] D. J. Moss, J. E. Sipe, and H. M. van Driel, Phys. Rev. B **36**, 9708 (1987).

[33] J. E. Sipe and A. I. Shkrebtii, Phys. Rev. B **61**, 5337 (2000).

[34] J. E. Sipe and E. Ghahramani, Phys. Rev. B **48**, 11705 (1993).

[35] Z. H. Levine and D. C. Allan, Phys. Rev. Lett. **63**, 1719 (1989).

[36] G. Strinati, Rivista del nuovo cimento **11**, 1 (1988).

[37] E. K. Chang, E. L. Shirley, and Z. H. Levine, Physical Review B **65**, 035205 (2001).

[38] R. Leitsmann, W. G. Schmidt, P. H. Hahn, and F. Bechstedt, Phys. Rev. B **71**, 195209 (2005).

[39] H. Hübener, Phys. Rev. A **83**, 062122 (2011).

[40] K. S. Virk and J. E. Sipe, Phys. Rev. B **80**, 165318 (2009).

[41] E. Runge and E. K. U. Gross, Phys. Rev. Lett. **52**, 997 (1984).

[42] S. Botti, A. Schindlmayr, R. Del Sole, and L. Reining, Reports on Progress in Physics **70**, 357 (2007).

[43] M. Cazzanelli, F. Bianco, E. Borga, G. Pucker, M. Ghulinyan, E. Degoli, E. Luppi, V. Véniard, S. Ossicini, D. Modotto, S. Wabnitz, R. Pierobon, and L. Pavesi, Nat. Mater. **11**, 148 (2012).

[44] S. Botti, F. Sottile, N. Vast, V. Olevano, L. Reining, H.-C. Weissker, A. Rubio, G. Onida, R. Del Sole, and R. Godby, Physical Review B **69**, 155112 (2004).

[45] I. Souza, J. Íñiguez, and D. Vanderbilt, Phys. Rev. B **69**, 085106 (2004).

[46] R. Resta, "Geometry and topology in electronic structure theory," .

[47] R. M. Martin and G. Ortiz, International Journal of Quantum Chemistry **69**, 567 (1998).

[48] R. D. King-Smith and D. Vanderbilt, Phys. Rev. B **47**, 1651 (1993).

[49] R. Resta, Phys. Rev. Lett. **80**, 1800 (1998).

[50] R. Resta, Rev. Mod. Phys. **66**, 899 (1994).

[51] R. Resta and S. Sorella, Physical Review Letters **82**, 370 (1999).

[52] G. Onida, L. Reining, and A. Rubio, Rev. Mod. Phys. **74**, 601 (2002).

[53] J. L. Cabellos, B. S. Mendoza, M. A. Escobar, F. Nastos, and J. E. Sipe, Phys. Rev. B **80**, 155205 (2009).

[54] G. Strinati, H. J. Mattausch, and W. Hanke, Phys. Rev. B **25**, 2867 (1982).

[55] C. Attaccalite, M. Grüning, and A. Marini, Phys. Rev. B **84**, 245110 (2011).

[56] W. Kohn and L. J. Sham, Phys. Rev. **140**, A1133 (1965).

[57] P. Hohenberg and W. Kohn, Phys. Rev. **136**, B864 (1964).

[58] C. Attaccalite and M. Grüning, Physical Review B **88**, 235113 (2013).

[59] L. Stella, C. Attaccalite, S. Sorella, and A. Rubio, Phys. Rev. B **84**, 245117 (2011).

[60] S. Massidda, R. Resta, M. Posternak, and A. Baldereschi, Phys. Rev. B **52**, R16977 (1995).

[61] K.-T. Chen and P. A. Lee, Phys. Rev. B **84**, 205137 (2011).

[62] A. Shitade, Journal of the Physical Society of Japan **83**, 033708 (2014).

[63] R. Nourafkan and G. Kotliar, Physical Review B **88**, 155121 (2013).

[64] D. Sangalli, Physical Review Materials **5**, 083803 (2021).

[65] W. G. Aulbur, L. Jönsson, and J. W. Wilkins, Solid State Physics (edited by H. Ehrenreich and F. Spaepen), Academic press **54**, 1 (1999).

[66] J. Li, N. D. Drummond, P. Schuck, and V. Olevano, SciPost Physics **6**, 040 (2019).

[67] X. Gonze, P. Ghosez, and R. Godby, Physical Review Letters **74**, 4035 (1995).

[68] N. Maitra, I. Souza, and K. Burke, Physical Review B **68**, 045109 (2003).

[69] S. K. Ghosh and A. K. Dhara, Phys. Rev. A **38**, 1149 (1988).

[70] M. Grüning, D. Sangalli, and C. Attaccalite, Phys. Rev. B **94**, 035149 (2016).

[71] M. Gruning and C. Attaccalite, Phys. Chem. Chem. Phys. **18**, 21179 (2016).

[72] C. Attaccalite, M. Grüning, H. Amara, S. Latil, and F. Ducastelle, Physical Review B **98**, 165126 (2018).

[73] H. Hübener, E. Luppi, and V. Véniard, Phys. Status Solidi B **427**, 1984 (2010).

[74] C. Attaccalite, A. Nguer, E. Cannuccia, and M. Grüning, Physical Chemistry Chemical Physics **17**, 9533 (2015).

[75] Y. Wei, X. Xu, S. Wang, W. Li, and Y. Jiang, Physical Chemistry Chemical Physics **21**, 21022 (2019).

[76] K. Beach, M. C. Lucking, and H. Terrones, Physical Review B **101**, 155431 (2020).

[77] H. Mishra and S. Bhattacharya, Physical Review B **101**, 155132 (2020).

[78] C. Attaccalite, M. Palummo, E. Cannuccia, and M. Grüning, Physical Review Materials **3**, 074003 (2019).

[79] C. Attaccalite, E. Cannuccia, and M. Grüning, Physical Review B **95**, 125403 (2017).

[80] D. Sangalli, A. Ferretti, H. Miranda, C. Attaccalite, I. Marri, E. Cannuccia, P. Melo, M. Marsili, F. Paleari, A. Marrazzo, *et al.*, Journal of Physics: Condensed Matter **31**, 325902 (2019).

[81] "Yambo wiki: non linear response," Yambo Wiki.

[82] W. Schafer and M. Wegener, *Semiconductor Optics and Transport Phenomena: From Fundamentals to Current Topics* (Springer, 2002).